Phosphate ion functionalization of perovskite surfaces for enhanced oxygen evolution reaction

Letter

Phosphate Ion Functionalization of Perovskites Surfaces for Enhanced Oxygen Evolution Reaction

Chunzhen Yang, Christel Laberty-Robert, Dmitry Batuk, Giannantonio Cibin, Alan V. Chadwick, Vanessa Pereira Pimenta, Wei Yin, Leiting Zhang, Jean-Marie Tarascon, and Alexis Grimaud

J. Phys. Chem. Lett., **Just Accepted Manuscript** • DOI: 10.1021/acs.jpclett.7b01504 • Publication Date (Web): 07 Jul 2017

Phosphate Ion Functionalization of Perovskites Surfaces for Enhanced Oxygen Evolution Reaction

Chunzhen Yang,[†] Christel Laberty-Robert,[‡] Dmitry Batuk,[§] Giannantonio Cibin,[∥] Alan V. Chadwick,[⊥] Vanessa Pereira Pimenta,[†] Wei Yin,[†] Leiting Zhang,[†] Jean-Marie Tarascon[†] and Alexis Grimaud*[,†]

[†] CNRS, UMR 8260 College de France, Paris, France

[‡] Sorbonne Universités – UPMC Univ. Paris 06, 4 place Jussieu, F-75005 Paris, France

[§] EMAT, University of Antwerp, Groenenborgerlaan 171, B-2020 Antwerp, Belgium

[∥] Diamond Light Source, Harwell Science and Innovation Campus, Didcot, Oxfordshire OX11 0DE, U.K.

[⊥] School of Physical Sciences, University of Kent, Canterbury, Kent CT2 7NH, U.K.

*Contact author information: alexis.grimaud@college-de-france.fr

Abstract

Recent findings revealed that surface oxygen can participate in the oxygen evolution reaction (OER) for the most active catalysts, which eventually triggers a new mechanism for which the deprotonation of surface intermediates limits the OER activity. We propose in this work a "dual strategy", for which tuning the electronic properties of the oxide such as $La_{1-x}Sr_xCoO_{3-\delta}$ can be dissociated from the use of surface functionalization with phosphate ion groups (Pi) that enhances the interfacial proton transfer. Results show that the P_i functionalized $La_{0.5}Sr_{0.5}CoO_{3-\delta}$ gives rise to a significant enhancement of the OER activity when compared to $La_{0.5}Sr_{0.5}CoO_{3-\delta}$ and $LaCoO_3$. We further demonstrate that the P_i surface functionalization selectivity enhances the activity when the OER kinetics is limited by the proton transfer. Finally, this work suggests that tuning the catalytic activity by such a "dual approach" may be a new and largely unexplored avenue for the design of novel high-performance catalysts.

TOC

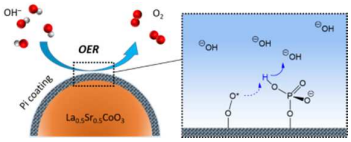

Developing highly active, cost-effective and stable catalysts for the oxygen evolution reaction (OER) is critical to improve the efficiency of many electrochemical technologies in pursuit of sustainable energy, such as water splitting using light or electricity, and rechargeable metal air batteries.[1-3] Recently, many transition-metal oxides (TMO) with the perovskite structure have been developed to promote the kinetics of the OER in alkaline electrolytes with comparable activities to precious-metal based catalysts such as state-of-the-art IrO_2 and RuO_2.[4-7] Nevertheless, the rational design of active catalysts is to date largely hampered by the lack of understanding of the exact mechanism for the OER on perovskite surfaces.

So-far, the generally adopted reaction mechanism for water electrocatalysis in alkaline media involves four consecutive proton-coupled electron transfer (PCET) steps on metal-ion centers for which oxygen molecules originate from adsorbed water molecules.[8-9] Optimizing the adsorption/desorption strength of reaction intermediates on catalyst surfaces, which must be neither too strong nor too weak, was proposed to have a significant impact for achieving high OER activities.[9-10] Following this approach, tuning the electronic properties of the perovskites has been studied as a strategy to control the adsorption strength.[4, 10]

Nevertheless, this commonly accepted mechanism is questioned by recent findings which revealed that, for the most active catalyst, oxygen is evolved not only by the oxidation of water but also by the direct oxidation of lattice oxygen.[11-15] Furthermore, triggering the redox activity of lattice oxygen was found to be associated with enhanced OER activity for cobalt-based perovskites such as $La_{1-x}Sr_xCoO_3$ (with $x \geq 0.5$).[11] More importantly, a shift in the rate determining step was suggested for oxides demonstrating lattice oxidation, this shift being associated with a strong pH dependence for the OER activity. Indeed, this dependence suggests a decoupled proton-electron transfer mechanism for which the rate determining step only involves proton.[8] Although studying the energetics of intermediates formed through a decoupled mechanism is challenging by the means of density functional theory (DFT) calculations, valuable insights could be reached. For instance, lowering the binding energy of OH^- on the surface of perovskites was shown to be correlated with a modification of the rate determining step, from the formation of O-O bond ($O_{(ads)} + OH^- \rightarrow OOH_{(ads)} + e^-$) for strong binding surfaces to the deprotonation of $OOH_{(ads)}$ ($OOH_{(ads)} + OH^- \rightarrow OO_{(ads)} + H^+ + e^-$) for weakly binding surfaces. In

conclusion, while experiments and theory reconcile in recognizing the importance of deprotonation steps for the most active catalysts, further work is needed to fully understand the complexity of the OER mechanism. Moreover, it is commonly admitted that the involvement of lattice oxygen in the OER is frequently associated with surface instabilities which therefore calls for the development of rational strategies.

Based on the current understanding, several strategies were proposed in the literature so to enhance the OER activity, such as tuning the oxygen or cation contents in perovskites,[16-17] developing nano-perovskites[18-19] or dimensionally stable anode[20]. In this work, we took another approach consisting in making surface functionalized catalysts, for which tuning the electronic structure of the bulk catalyst would lower the energy for forming the O-O bond and a functionalized surface would improve the interfacial proton transfer, appears to be a promising "dual strategy". The general requirements for making a successful surface functionalization and to effectively improve the interfacial proton transfer can be summarized as follow: *(1)* having a *pK*a below the pH of the solution, *(2)* being stable under the operative conditions and *(3)* being porous so water can reach the surface of the catalyst. Phosphate coating (P_i), which had been well explored for other applications such as molecular organics, can be a promising choice to demonstrate this bi-functional strategy.[21-22] Indeed, PO_4^{3-} groups possess a well-adapted pKa (12.67) and strong nucleophilic property.[23] The perovskite $LaCoO_3$ (denoted as LCO) is often considered as a compound of reference since it was demonstrated to have no pH dependence and to follow a classical PCET mechanism.[11] In contrary, Sr^{2+}-substituted $La_{0.5}Sr_{0.5}CoO_{3-\delta}$ (denoted as LSC) was previously shown to possess a large pH dependence for the OER activity, suggesting a rate determining step for which only protons are involved.[11] Therefore, designing surface functionalized catalysts using these two model catalysts with phosphate functional groups can give further insights into the OER mechanism. Coupling the pH dependence study with isotopic measurements replacing H_2O by D_2O will further provide a better understanding of the proton transfer kinetics on the surface of perovskites during OER.[24] At last, the stability of the surface upon cycling, which is critical to enable the use of such catalyst in real devices, will be assessed.

The surface functionalization of perovskites was conducted following a procedure previously reported.[25] The P_i coating was first characterized by the means of X-ray diffraction (XRD), X-ray photoelectron spectroscopy (XPS), X-ray absorption spectroscopy (XAS) and Infrared spectroscopy (IR) to examine that the surface functionalization 1) doesn't modify the crystalline structure of perovskite and 2) is uniform. XRD spectra reported in Figure 1a revealed that the crystallinity of the perovskites LCO and LSC is kept after coating with P_i (Figure S1 and Table S1). Characteristic vibrations from P-O bond and PO_4^{3-} groups (1000 cm^{-1} and 700 cm^{-1}, respectively) are identified by IR spectroscopy (Figure S2). It confirms the successful functionalization of the oxide surface with P_i functional groups which is further demonstrating by the means of XPS spectra for LSC and LSC-Pi (Figure 1b). Hence, appearance of a strong peak in the P 2p signal at 133.8 eV on the coated LSC- P_i sample is observed while a decrease of the relative intensity for peaks related to lattice Sr^{2+} is observed.[26] Furthermore, no noticeable modification of the Co 2p peaks can be seen, suggesting no reduction or oxidation of the surface following the functionalization with PO_4^{3-}.[27]

XAS measurements at the Co K-edge were then performed in the surface sensitive total electron yield (TEY) mode so to definitively demonstrate that the surface of the perovskite is not affected by the P_i surface functionalization.[28] Both X-ray absorption near edge structure (XANES) and extended X-ray absorption fine structure (EXAFS) parts were analyzed to probe the Co oxidation state and the local structure on the surface of the catalysts, respectively (Figures 1c and 1d). The positions of the Co K-edge for pristine and functionalized LCO at 7725.9 eV indicate that the oxidation states of Co ion remains unchanged (Co^{3+}) with the P_i functionalization. In a similar manner, the Co K-edge spectra recorded for LSC and LSC-Pi doesn't evidence any surface oxidation or reduction induced by the functionalization, while the energy of the edge (7727.2 eV) indicates a partial oxidation of cobalt when compared to LCO ($Co^{3.5+}$ as given by the stoichiometry).[29] The k^3-weighted Fourier-transform (FT)-EXAFS spectra further indicates the preserved CoO_6 octahedral unit, with a slight elongation of the Co-O bonds for functionalized samples probably due to the formation of metal-oxo bond between cobalt and PO_4^{3-} groups.

At last, elemental mapping (Figure 1e) obtained by scanning transmission electron microscopy (STEM) with energy dispersive X-ray spectrometry (EDS) definitively

confirmed that trace amount of phosphate (0.58 a.t.%) are uniformly covering the surface of perovskites (Figure S3). All elements were perfectly distributed and no region was found with segregation of Co and P atoms on the surface, which excludes the formation of the well-known CoP_i amorphous catalysts during coating.

Based on the above described characterizations, bi-functional catalysts were successfully designed for which the surface of the perovskites is functionalized with phosphate while their chemical and structural structures are unaltered. More importantly, no secondary phase was formed at the interface between the oxide and the phosphate.

The electrocatalytic activity of pristine and functionalized perovskites was examined by cyclic voltammetry (CV) (Figure 2). In 0.1 M KOH solution (pH=13), the OER activities can be ranked in the order of LSC–P_i > LSC > LCO–P_i ~ LCO. The P_i-functionalized LSC surface effectively improves the OER currents, which is approximately two times higher than that of the pristine one, and one order of magnitude higher compared to LCO. Furthermore, the P_i surface functionalization doesn't modify the OER activity for LCO. Hence, the design of P_i-functionalized catalysts only selectively enhances the OER activity.

To understand this selectivity, the OER activities were further compared at different pH for the pristine and functionalized LCO and LSC. Tafel plots are given in Figure S4. As shown in Figure 2a, the OER currents were found to increase with increasing pH for both LSC and LSC–Pi, but remained unchanged for LCO and LCO–P_i. The results obtained for pristine LSC and LCO is consistent with previous report.[11] The dependence of the reaction rate on the proton activity was derived based on the following equation:

$$\rho_{RHE} = \left(\frac{\partial \log(j)}{\partial pH}\right)_E = -\left(\frac{\partial E}{\partial \log(j)}\right)_{pH} / \left(\frac{\partial E}{\partial pH}\right)_j$$

with ρ_{RHE} being the proton reaction order on the RHE scale.[30] From the extracted slopes, the proton reaction orders are therefore estimated to be 0.49, 0.76, 0.15 and 0.12 for LSC-Pi, LSC, LCO-Pi and LCO, respectively.

Combining experimental results with previous computational reports, the strong pH dependent behavior could indicate: 1) a change of rate limiting step (RLS) from the O-O bond formation, typically expected for LCO, to the subsequent step of deprotonation of OOH species for LSC, and 2) that this deprotonation step is

decoupled.[11] Assuming the OOH deprotonation to be RLS, the OER current can be expressed as $i = [OH^-] \cdot \theta \cdot e^{-\frac{DG}{RT}}$, with θ being the surface coverage of the adsorbed *OOH sites and [OH^-] the concentration in solution. Therefore, increasing the pH can either increase the pre-exponential term by simply increasing the concentration of OH^-, or the surface coverage, or can also alter the exponential term by modifying the energy of the adsorbed *OOH and OO^- intermediates. Bearing in mind that, in addition to the enhanced OER current, the Tafel slope was found to decrease when coating the surface of LSC (Figure S4), one can propose that increasing the pH has both effects.[31] Finally, we could demonstrate that the OER enhancement for the coated surfaces is not limited to the pH range 12.5-14, but also occurs at near neutral pH of 10.6 in buffered solution (Figure S6).

In conclusion, the surface P_i functionalization improves the performance of LSC by presumably enhancing the kinetics of the proton transfer at the catalysts/water interface. Aware of this, it becomes obvious that the P_i functionalization demonstrates a greater effect at low pH where the proton transfer is very slow, but that the effect is reduced at higher pH where the driving force for the proton exchange is much greater.

To gain deeper insights on the proton transfer at the interface between P_i groups/perovskite/water, we further use isotopic labelling and compare measurements carried out in D_2O and H_2O solutions. Suh an approach was inspired by biological studies on the structure of proteins where H/D exchange is used to probe the hydrogen bonding network and the solvent accessibility, so to explore the tertiary structure of the protein, the folding pathways and other phenomena.[32-34] Since proton mobility in deuterated water solutions can be 1.6 to 5.0 times slower than that in various protonated water electrolytes[35], the use of D_2O as a testing media can effectively slow down the proton transfer kinetics.

Electrochemical results comparing the OER activities in KOH/H_2O and KOH/D_2O are shown in Figure 3 for uncoated LCO and LSC. As expected, LCO was found to be almost insensitive to the use of D_2O (0.08 mA cm^{-2} in H_2O vs. 0.07 mA cm^{-2} in D_2O measured at 0.85 V vs. NHE). In contrary, LSC shows a strong H/D isotopic effect with the OER current measured in D_2O being significantly decreased (0.42 mA cm^{-2} in H_2O vs. 0.19 mA cm^{-2} in D_2O measured at 0.85 V vs. NHE). Moreover, Tafel slopes derived from the OER curves also largely increased from 98 mV dec^{-1} to 130

mV dec^{-1} when using D_2O solution. For the LSC-P_i sample, the H/D effect becomes weaker which demonstrates that the interfacial proton transfer is enhanced when mediated by the phosphate groups. Nevertheless, with increasing current densities, the OER activity eventually decreases when using D_2O, indicating that the interfacial proton transfer mediated by the phosphate groups becomes eventually limiting at higher rate. Overall, a slight increase of the Tafel slope from 90 mV dec^{-1} to 99 mV dec^{-1} is observed when replacing H_2O by D_2O, further suggesting that the energies of the intermediate controlling the reaction is largely dependent on the hydrogen bond network as well as on the dynamics of the proton.

Altogether, our surface functionalization strategy combined with the pH dependence measurements and our H/D isotopic exploration provide valuable insights concerning the OER mechanism on the surface of perovskite which will be discussed below.

Although triggering the redox activity of lattice oxygen by lowering the Fermi level closer to the O *p*-states can effectively promote the catalytic activity, it is often associated with increasing instability for perovskite surfaces.[4, 14, 36] Hence, several very active perovskites, such as $Ba_{0.5}Sr_{0.5}Co_{0.8}Fe_{0.2}O_{3-\delta}$ (BSCF), or else, have been reported to undergo rapid surface amorphization and drastic structural oscillations during the OER.[4, 37] It is therefore worth examining the stability of the P_i-functionalized surfaces developed in this work. For that, the LSC-P_i sample was subjected to a long cycling test within a potential range of 1.1-1.7 V vs. RHE in 0.1 M KOH solution (Figure 4). While uncoated LSC shows activity fade upon cycling (Figure S8), the P_i-functionalized catalyst demonstrates stable electrocatalytic current throughout the test (Figure 4a). Looking in details into the CV curves (Figure 4b), no drastic increase of the capacitive region was observed, in contrary to unstable perovskites such as BSCF for instance.[38] Nevertheless, a broad redox peak was very gradually formed at ~1.45 V vs. RHE, which could eventually be attributed to the typical Co redox observed for amorphous cobalt hydroxide species.[39] We therefore further investigated the bulk and surface stability of this catalyst by combining XRD and XAS, respectively.

First, the XRD spectra for the cycled catalysts show no degradation, demonstrating the bulk stability for the coated perovskite catalyst (Figure S11). XAS was then conducted at the Co K-edge in the surface sensitive TEY mode to study the evolution

of the local structure on the surface during the cycling. The Co K-edge position was found stable after cycling for 10 and 50 cycles, which indicates no significant modifications of the Co oxidation state upon cycling (Figure 4c). The motifs observed in the $k_3\chi(k)$ EXAFS spectra are the fingerprint of the perovskites structure and correspond from the lower reduced distance to the greater reduced distance to the Co-O, Co-La(Sr) and Co-Co bonds, respectively (Figure 4d). No drastic changes were observed upon cycling for Pi-LSC, and more precisely no peaks associated to the formation of edge-shared octahedral motifs (reduced distance of 1.7-1.8 Å) corresponding to the formation of an amorphous cobalt oxyhydroxide surface was detected.[40-41] This further confirmed the stability of the interface between the phosphate coating and the surface of the oxide.

In light of the above results, we proposed a "dual strategy" (Figure 5) that consists in tuning the electronic structure of perovskites OER catalyst so as to lower the O-O bond energy barrier formation and using P_i functional group to improve the interfacial proton transfer.

We first verify that the selective enhancement of the OER activity following the surface functionalization does not originate from the presence of phosphate groups in solution, rather than from the P_i functional group itself. We therefore further measured the OER activity in a series of KOH/K_3PO_4 buffer solutions with different concentrations of $[P_i]$ (increasing from 0 to 50, 100, 200 and 500 mM) at a fixed pH of 13. We could confirm that introducing the phosphate anions into the electrolyte does not promote the OER activities for perovskites (Figure S12), ruling out the role of phosphate groups in solution as the origin for the enhanced OER activity. This conclusion is in agreement with previous report from Ullman et al. who reported a zero order dependence of $[P_i]$ concentration on the OER activity for Co-based oxygen evolving catalysis.[42] Moreover, Andrew et al. attributed this zero order dependence of $[P_i]$ concentration in solution to the slow P_i binding kinetics on the cobalt(III) edge sites.[42] On the other hand, Hunter et. al. found that the OER activity of Ni-Fe layered double hydroxide was correlated with the pK_a of the conjugated acid for different interlayer anions.[23] Among various anions, including PO_4^{3-}, NO_3^-, CO_3^{2-}, Cl^-, SO_4^{2-} and others, PO_4^{3-} demonstrated the largest enhancement due to its high pKa (12.67) and its strong nucleophilic property. Combining these previous results with

our experimental results, it can be anticipated that anchoring P_i groups onto the electrocatalytically active interface can be a unique strategy for improving the interfacial proton dynamics and the catalytic activity.

Understanding why the P_i surface functionalization can selectively enhance the OER activities for perovskites then becomes of prime importance. As being discussed in several recent studies, perovskites such as LCO presumably catalyze water oxidation via four consecutive PCET steps with the O-O bond formation being the RLS.[5] Therefore, the catalytic activity for LCO is largely depending on the adsorption strength of OH^- onto the metal sites. By tuning its electronic structure through Sr^{2+} substitution, key parameters including the oxygen vacancies, Co-O bond covalency and redox activity of lattice oxygen species can be optimized.[5, 43-45] For several perovskites with enhanced activity, such as $SrCoO_{3-\delta}$, $Pr_{0.5}Ba_{0.5}CoO_{3-\delta}$, LSC and others, it was then proposed that their reactive centers become the surface oxygen, rather than the metallic sites. This can be explained by the oxidation of the lattice oxygen upon OER condition, making them electrophilic and reactive with either lone pair electrons from water (acid-base mechanism) or with other surface oxygen (direct coupling mechanism). Overall, this oxidation process eventually lowers the energy barriers for the O-O bond formation,[4, 11, 14] which triggers a change in RLS from the O-O bond formation to a deprotonation step. Moreover, not only the RLS change, but the deprotonation step becomes largely dependent on the proton kinetics, resulting in a strong pH dependence and H/D isotope sensitivity as demonstrated in this work. Therefore, the P_i surface functionalization of these perovskites could be a promising strategy to enhance the OER activities for such catalysts since the enriched proton network between PO_4^{3-}/oxide/water improves the interfacial proton transfer kinetics within the inner Helmholtz plane.

In conclusion, we proposed in this work a "dual strategy" where antagonist properties such as the electronic structure of the perovskites and the interfacial proton transfer kinetics can be independently tuned. We thoroughly investigated the origin for the improved OER activity with P_i surface functionalization by combining a pH dependence study with D_2O measurements. We could demonstrate that the P_i functional groups selectively improved the OER for perovskites that are showing high pH dependence related to limited proton transfer kinetics. In particular, the LSC-P_i

sample exhibits OER activity ≈ 10 times greater when compared to that of LCO. We could also demonstrate that the coating strategy doesn't bring additional instability, and could actually be a valuable strategy to improve surface stability. Hence, these results provide additional experimental supports for the previously proposed "non-concerted" OER mechanism that is triggered by the lattice oxygen oxidation and which is fundamentally different from the classical concerted mechanism. It also suggests that engineering the interface of electrocatalysts requires a proper understanding of the underlying reaction mechanism. At last, it is worth pointing out that combining pH dependence study and D_2O measurement can be a powerful electrochemical strategy to investigate the PCET mechanism on electrocatalyst interfaces. This method can be well adopted to explore other electrocatalyst systems involving proton transfer, such as H_2 evolution, CO_2 reduction, alcohol oxidation and many others.

Supporting Information Available: Supporting information includes experimental details, physical characterizations, such as XRD, IR, SEM and EDS analyses, and more electrochemistry analyses. This material is available free of charge via the Internet http://pubs.acs.org.

Acknowledgement

C.Y., J.-M.T. and A.G. acknowledge funding from the European Research Council (ERC) (FP/2014)/ERC Grant-Project 670116-ARPEMA. We acknowledge Diamond Light Source for time awarded to the Energy Materials BAG on Beamline B18, under proposal sp12559.

References

(1) Hong, W. T.; Risch, M.; Stoerzinger, K. A.; Grimaud, A.; Suntivich, J.; Shao-Horn, Y. Toward the Rational Design of Non-Precious Transition Metal Oxides for Oxygen Electrocatalysis. *Energy Environ. Sci.* **2015**, *8*, 1404-1427.

(2) Hunter, B. M.; Gray, H. B.; Muller, A. M. Earth-Abundant Heterogeneous Water Oxidation Catalysts. *Chem. Rev.* **2016**.

(3) Dau, H.; Limberg, C.; Reier, T.; Risch, M.; Roggan, S.; Strasser, P. The Mechanism of Water Oxidation: From Electrolysis Via Homogeneous to Biological Catalysis. *ChemCatChem* **2010**, *2*, 724-761.

(4) Grimaud, A.; May, K. J.; Carlton, C. E.; Lee, Y. L.; Risch, M.; Hong, W. T.; Zhou, J.; Shao-Horn, Y. Double Perovskites as a Family of Highly Active Catalysts for Oxygen Evolution in Alkaline Solution. *Nat. Commun.* **2013**, *4*, 2439.

(5) Mefford, J. T.; Rong, X.; Abakumov, A. M.; Hardin, W. G.; Dai, S.; Kolpak, A. M.; Johnston, K. P.; Stevenson, K. J. Water Electrolysis on $La_{1-x}Sr_xCoO_{3-\delta}$ Perovskite Electrocatalysts. *Nat. Commun.* **2016**, *7*, 11053.

(6) Risch, M.; Stoerzinger, K. A.; Maruyama, S.; Hong, W. T.; Takeuchi, I.; Shao-Horn, Y. $La_{0.8}Sr_{0.2}MnO_{3-\delta}$ decorated with $Ba_{0.5}Sr_{0.5}Co_{0.8}Fe_{0.2}O_{3-\delta}$: A Bifunctional Surface for Oxygen Electrocatalysis with Enhanced Stability and Activity. *J. Am. Chem. Soc.* **2014**, *136*, 5229-5232.

(7) Yagi, S.; Yamada, I.; Tsukasaki, H.; Seno, A.; Murakami, M.; Fujii, H.; Chen, H.; Umezawa, N.; Abe, H.; Nishiyama, N. *et al.* Covalency-reinforced oxygen evolution reaction catalyst. *Nat. Commun.* **2015**, *6*, 8249.

(8) Koper, M. T. M. Theory of Multiple Proton–Electron Transfer Reactions and Its Implications for Electrocatalysis. *Chem. Sci.* **2013**, *4*, 2710.

(9) Man, I. C.; Su, H.-Y.; Calle-Vallejo, F.; Hansen, H. A.; Martínez, J. I.; Inoglu, N. G.; Kitchin, J.; Jaramillo, T. F.; Nørskov, J. K.; Rossmeisl, J. Universality in Oxygen Evolution Electrocatalysis on Oxide Surfaces. *ChemCatChem* **2011**, *3*, 1159-1165.

(10) Suntivich, J.; May, K. J.; Gasteiger, H. A.; Goodenough, J. B.; Shao-Horn, Y. A Perovskite Oxide Optimized for Oxygen Evolution Catalysis from Molecular Orbital Principles. *Science* **2011**, *334*, 1383-1385.

(11) Grimaud, A.; Diaz-Morales, O.; Han, B.; Hong, W. T.; Lee, Y. L.; Giordano, L.; Stoerzinger, K. A.; Koper, M. T. M.; Shao-Horn, Y. Activating Lattice Oxygen Redox Reactions in Metal Oxides to Catalyse Oxygen Evolution. *Nat. Chem.* **2017**, *9*, 457-465.

(12) Grimaud, A.; Demortiere, A.; Saubanere, M.; Dachraoui, W.; Duchamp, M.; Doublet, M.-L.; Tarascon, J.-M. Activation of Surface Oxygen Sites on an Iridium-Based Model Catalyst for the Oxygen Evolution Reaction. *Nat. Energy*

2016, *2*, 16189.

(13) Grimaud, A.; Hong, W. T.; Shao-Horn, Y.; Tarascon, J. M. Anionic Redox Processes for Electrochemical Devices. *Nat. Mater.* **2016**, *15*, 121-6.

(14) Rong, X.; Parolin, J.; Kolpak, A. M. A Fundamental Relationship between Reaction Mechanism and Stability in Metal Oxide Catalysts for Oxygen Evolution. *ACS Catalysis* **2016**, *6*, 1153-1158.

(15) Yang, C.; Grimaud, A. Factors Controlling the Redox Activity of Oxygen in Perovskites: From Theory to Application for Catalytic Reactions. *Catalysts* **2017**, *7*, 149.

(16) Petrie, J. R.; Jeen, H.; Barron, S. C.; Meyer, T. L.; Lee, H. N. Enhancing Perovskite Electrocatalysis through Strain Tuning of the Oxygen Deficiency. *J. Am. Chem. Soc.* **2016**, *138*, 7252-7255.

(17) Zhu, Y.; Zhou, W.; Yu, J.; Chen, Y.; Liu, M.; Shao, Z. Enhancing Electrocatalytic Activity of Perovskite Oxides by Tuning Cation Deficiency for Oxygen Reduction and Evolution Reactions. *Chem. Mater.* **2016**, *28*, 1691-1697.

(18) Hardin, W. G.; Slanac, D. A.; Wang, X.; Dai, S.; Johnston, K. P.; Stevenson, K. J. Highly Active, Nonprecious Metal Perovskite Electrocatalysts for Bifunctional Metal–Air Battery Electrodes. *J. Phys. Chem. Lett.* **2013**, *4*, 1254-1259.

(19) Zhao, B.; Zhang, L.; Zhen, D.; Yoo, S.; Ding, Y.; Chen, D.; Chen, Y.; Zhang, Q.; Doyle, B.; Xiong, X. *et al.* A tailored double perovskite nanofiber catalyst enables ultrafast oxygen evolution. *Nat. Commun.* **2017**, *8*, 14586.

(20) Lyons, M. E. G.; Doyle, R. L.; Fernandez, D.; Godwin, I. J.; Browne, M. P.; Rovetta, A. The Mechanism and Kinetics of Electrochemical Water Oxidation at Oxidized Metal and Metal Oxide Electrodes. Part 1. General Considerations: A Mini Review. *Electrochem. Commun.* **2014**, *45*, 60-62.

(21) Paniagua, S. A.; Giordano, A. J.; Smith, O. L.; Barlow, S.; Li, H.; Armstrong, N. R.; Pemberton, J. E.; Bredas, J. L.; Ginger, D.; Marder, S. R. Phosphonic Acids for Interfacial Engineering of Transparent Conductive Oxides. *Chem. Rev.* **2016**, *116*, 7117-58.

(22) Li, Y.; Zhao, C. Enhancing Water Oxidation Catalysis on a Synergistic Phosphorylated Nife Hydroxide by Adjusting Catalyst Wettability. *ACS Catalysis* **2017**, 2535-2541.

(23) Hunter, B. M.; Hieringer, W.; Winkler, J. R.; Gray, H. B.; Müller, A. M. Effect of Interlayer Anions on [Nife]-Ldh Nanosheet Water Oxidation Activity. *Energy Environ. Sci.* **2016**, *9*, 1734-1743.

(24) Yang, C.; Fontaine, O.; Tarascon, J.-M.; Grimaud, A. Chemical Recognition of Active Oxygen Species on the Surface of Oxygen Evolution Reaction Electrocatalysts. *Angewandte Chem.* **2017**.

(25) Kim, J. Y.; Jang, J.-W.; Youn, D. H.; Magesh, G.; Lee, J. S. A Stable and Efficient Hematite Photoanode in a Neutral Electrolyte for Solar Water Splitting: Towards Stability Engineering. *Adv. Energy Mater.* **2014**, *4*, 1400476.

(26) Mutoro, E.; Crumlin, E. J.; Biegalski, M. D.; Christen, H. M.; Shao-Horn, Y. Enhanced Oxygen Reduction Activity on Surface-Decorated Perovskite Thin Films for Solid Oxide Fuel Cells. *Energy Environ. Sci.* **2011**, *4*, 3689.

(27) Cai, Z.; Xu, W.; Li, F.; Yao, Q.; Chen, X. Electropolymerization Fabrication of Co Phosphate Nanoparticles Encapsulated in N,P-Codoped Mesoporous Carbon Networks as a 3d Integrated Electrode for Full Water Splitting. *ACS Sustainable Chem. Eng.* **2017**, *5*, 571-579.

(28) Fauth, K. How Well Does Total Electron Yield Measure X-Ray Absorption in Nanoparticles? *Appl. Phys. Lett.* **2004**, *85*, 3271-3273.

(29) Hadt, R. G.; Hayes, D.; Brodsky, C. N.; Ullman, A. M.; Casa, D. M.; Upton, M. H.; Nocera, D. G.; Chen, L. X. X-Ray Spectroscopic Characterization of Co(IV) and Metal–Metal Interactions in Co_4O_4: Electronic Structure Contributions to the Formation of High-Valent States Relevant to the Oxygen Evolution Reaction. *J. Am. Chem. Soc.* **2016**, *138*, 11017-11030.

(30) Giordano, L.; Han, B.; Risch, M.; Hong, W. T.; Rao, R. R.; Stoerzinger, K. A.; Shao-Horn, Y. pH Dependence of OER Activity of Oxides: Current and Future Perspectives. *Catal. Today* **2016**, *262*, 2-10.

(31) Shinagawa, T.; Garcia-Esparza, A. T.; Takanabe, K. Insight on Tafel Slopes from a Microkinetic Analysis of Aqueous Electrocatalysis for Energy Conversion. *Sci. Rep.* **2015**, *5*, 13801.

(32) Cioni, P.; Strambini, G. B. Effect of Heavy Water on Protein Flexibility. *Biophys. J.* **2002**, *82*, 3246-3253.

(33) Maybury, R. H.; Katz, J. J. Protein Denaturation in Heavy Water. *Nature* **1956**, *177*, 629-630.

(34) Konermann, L.; Pan, J.; Liu, Y.-H. Hydrogen Exchange Mass Spectrometry for Studying Protein Structure and Dynamics. *Chem. Soc. Rev.* **2011**, *40*, 1224-1234.

(35) Roberts, N. K.; Northey, H. L. Proton and Deuteron Mobility in Normal and Heavy Water Solutions of Electrolytes. *J. Chem. Soc., Faraday Transactions 1: Physical Chemistry in Condensed Phases* **1974**, *70*, 253.

(36) Spoeri, C.; Kwan, J. T. H.; Bonakdarpour, A.; Wilkinson, D.; Strasser, P. The Stability Challenges of Oxygen Evolving Electrocatalysts: Towards a Common Fundamental Understanding and Mitigation of Catalyst Degradation. *Angew. Chem.* **2016**.

(37) Han, B.; Stoerzinger, Kelsey A.; Tileli, V.; Gamalski, Andrew D.; Stach, Eric A.;

Shao-Horn, Y. Nanoscale Structural Oscillations in Perovskite Oxides Induced by Oxygen Evolution. *Nat. Mater.* **2016**, *16*, 121-126.

(38) May, K. J.; Carlton, C. E.; Stoerzinger, K. A.; Risch, M.; Suntivich, J.; Lee, Y.-L.; Grimaud, A.; Shao-Horn, Y. Influence of Oxygen Evolution During Water Oxidation on the Surface of Perovskite Oxide Catalysts. *J. Phys. Chem. Lett.* **2012**, *3*, 3264-3270.

(39) Gerken, J. B.; McAlpin, J. G.; Chen, J. Y.; Rigsby, M. L.; Casey, W. H.; Britt, R. D.; Stahl, S. S. Electrochemical Water Oxidation with Cobalt-Based Electrocatalysts from pH 0-14: The Thermodynamic Basis for Catalyst Structure, Stability, and Activity. *J. Am. Chem. Soc.* **2011**, *133*, 14431-42.

(40) Risch, M.; Grimaud, A.; May, K. J.; Stoerzinger, K. A.; Chen, T. J.; Mansour, A. N.; Shao-Horn, Y. Structural Changes of Cobalt-Based Perovskites Upon Water Oxidation Investigated by Exafs. *J. Phys. Chem. C* **2013**, *117*, 8628-8635.

(41) Risch, M.; Khare, V.; Zaharieva, I.; Gerencser, L.; Chernev, P.; Dau, H. Cobalt−Oxo Core of a Water-Oxidizing Catalyst Film. *J. Am. Chem. Soc.* **2009**, *131*, 6936-6937.

(42) Ullman, A. M.; Brodsky, C. N.; Li, N.; Zheng, S. L.; Nocera, D. G. Probing Edge Site Reactivity of Oxidic Cobalt Water Oxidation Catalysts. *J. Am. Chem. Soc.* **2016**.

(43) Mueller, D. N.; Machala, M. L.; Bluhm, H.; Chueh, W. C. Redox Activity of Surface Oxygen Anions in Oxygen-Deficient Perovskite Oxides During Electrochemical Reactions. *Nat. Commun.* **2015**, *6*, 6097.

(44) Cheng, X.; Fabbri, E.; Nachtegaal, M.; Castelli, I. E.; El Kazzi, M.; Haumont, R.; Marzari, N.; Schmidt, T. J. Oxygen Evolution Reaction on $La_{1-X}Sr_xCoO_3$ perovskites: A Combined Experimental and Theoretical Study of Their Structural, Electronic, and Electrochemical Properties. *Chem. Mater.* **2015**, *27*, 7662-7672.

(45) Merkle, R.; Mastrikov, Y. A.; Kotomin, E. A.; Kuklja, M. M.; Maier, J. First Principles Calculations of Oxygen Vacancy Formation and Migration in $Ba_{1-X}Sr_xCo_{1-Y}Fe_yO_{3-\delta}$ Perovskites. *J. Electrochem. Soc.* **2012**, *159*, B219.

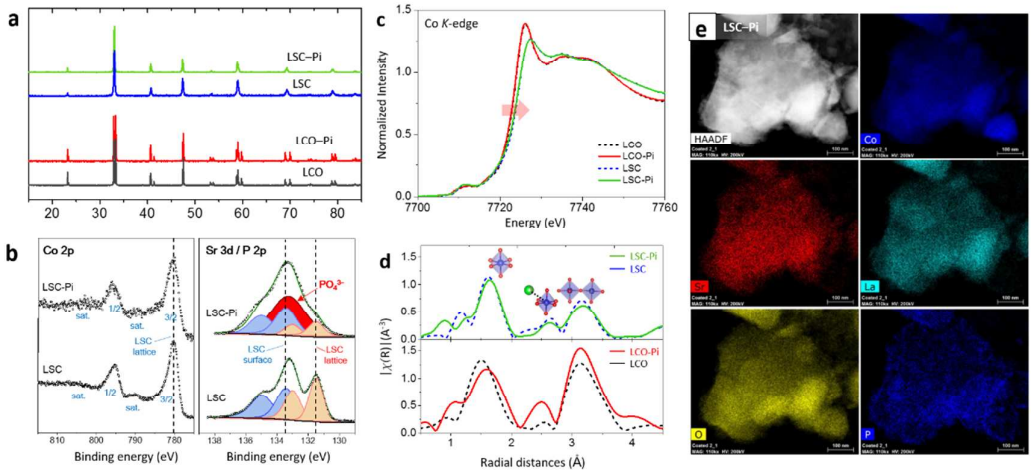

Figure 1. Surface functionalization of perovskite oxides with phosphate (P_i) groups. (a) XRD patterns of the pristine and the functionalized $LaCoO_3$, $La_{0.5}Sr_{0.5}CoO_{3-\delta}$ catalysts. (b) XPS analyses of the Co 2*p* (c) and P 2*p* and Sr 3*s* for the pristine and coated $La_{0.5}Sr_{0.5}CoO_{3-\delta}$ catalysts. (c) Co K-edge XANES profiles of the pristine and the functionalized $LaCoO_3$, $La_{0.5}Sr_{0.5}CoO_{3-\delta}$ catalysts. (d) k^3-weighted Fourier-transform (FT)-EXAFS spectra. (e) HRTEM image and EDS elemental maps of the surface functionalized $La_{0.5}Sr_{0.5}CoO_3$-P_i, demonstrating an even distribution of cobalt, strontium, lanthanum, oxygen and phosphorus elements in sample particles.

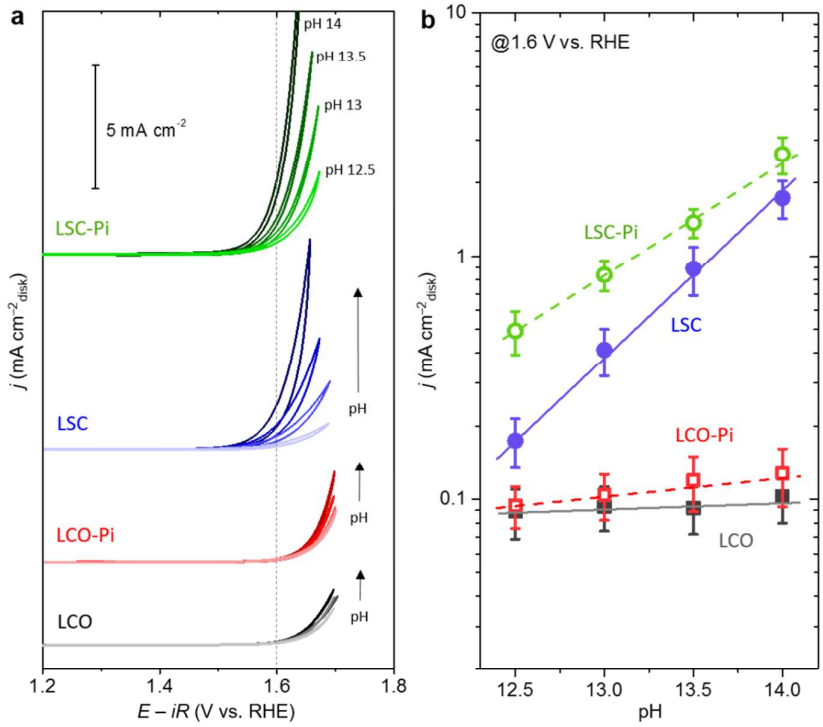

Figure 2. pH dependence of the OER activity. (a) CV curves of the $La_{0.5}Sr_{0.5}CoO_{3-\delta}$-$P_i$ (green), $La_{0.5}Sr_{0.5}CoO_{3-\delta}$ (blue), $LaCoO_3$-P_i (red) and $LaCoO_3$ (gray) in KOH solutions with pH increasing from 12.5 to 14. (b) Comparison of the current densities measured at 1.6 V vs. RHE at different pH.

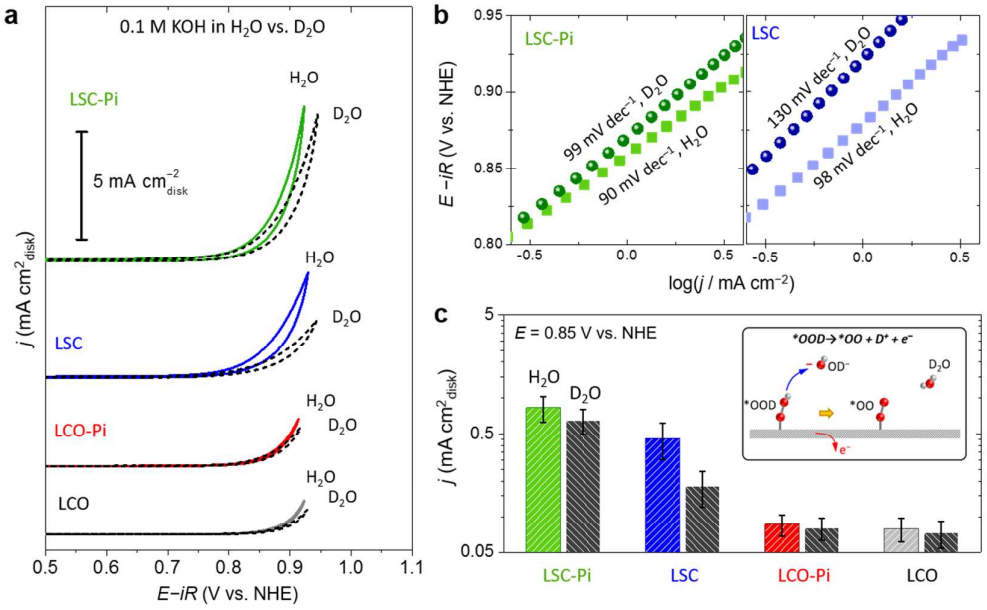

Figure 3. H/D isotope effect measurement. (a) OER activities of $La_{0.5}Sr_{0.5}CoO_{3-\delta}$-$P_i$, $La_{0.5}Sr_{0.5}CoO_{3-\delta}$, $LaCoO_3$-P_i and $LaCoO_3$ measured in 0.1 M KOH in H_2O and D_2O. (b) Comparison of Tafel plots of $La_{0.5}Sr_{0.5}CoO_{3-\delta}$-$P_i$ and $La_{0.5}Sr_{0.5}CoO_{3-\delta}$ measured in H_2O and D_2O. (c) Comparison of the current densities measured at 0.85 V vs. NHE. Inset illustrates the deprotonation process of adsorbed –OOD to –OO* on perovskite surface. Using D_2O as solvent effectively slows down the proton diffusion kinetics on the electrolyte/catalyst interface.

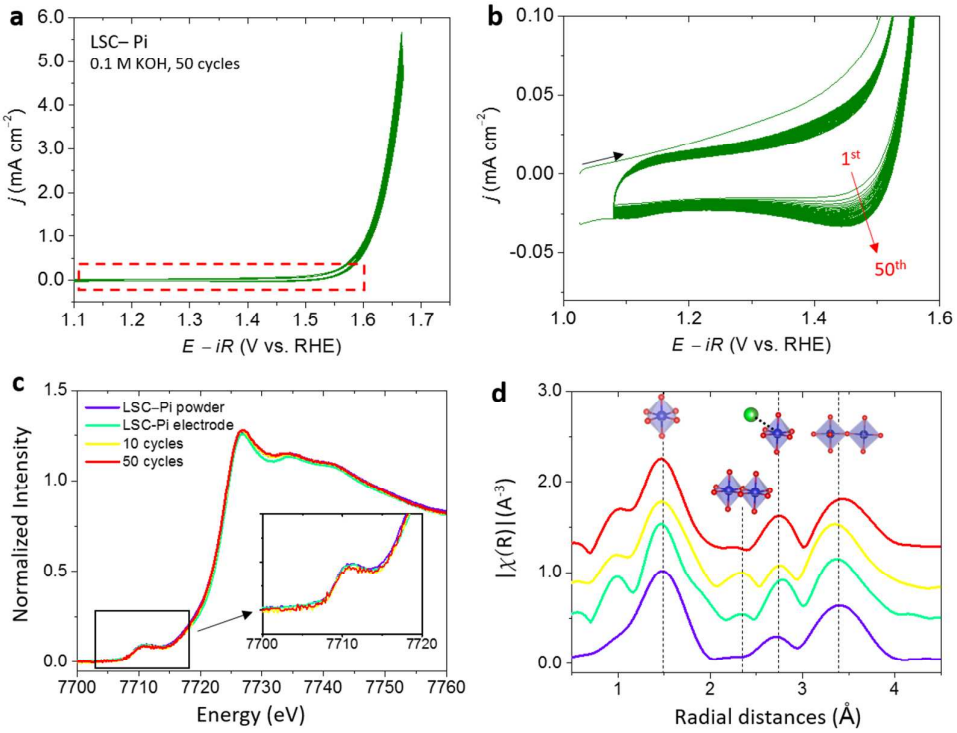

Figure 4. Cycling stability test for the $La_{0.5}Sr_{0.5}CoO_{3-\delta}$-$P_i$ catalyst. (a-b) CV curves for 50 cycles tested in 0.1 M KOH solution. (c) Co K-edge XANES spectra of the as-synthesized and cycled $La_{0.5}Sr_{0.5}CoO_{3-\delta}$-$P_i$ catalysts. (d) Oscillations of the k^3-weighted FT-EXAFS spectra.

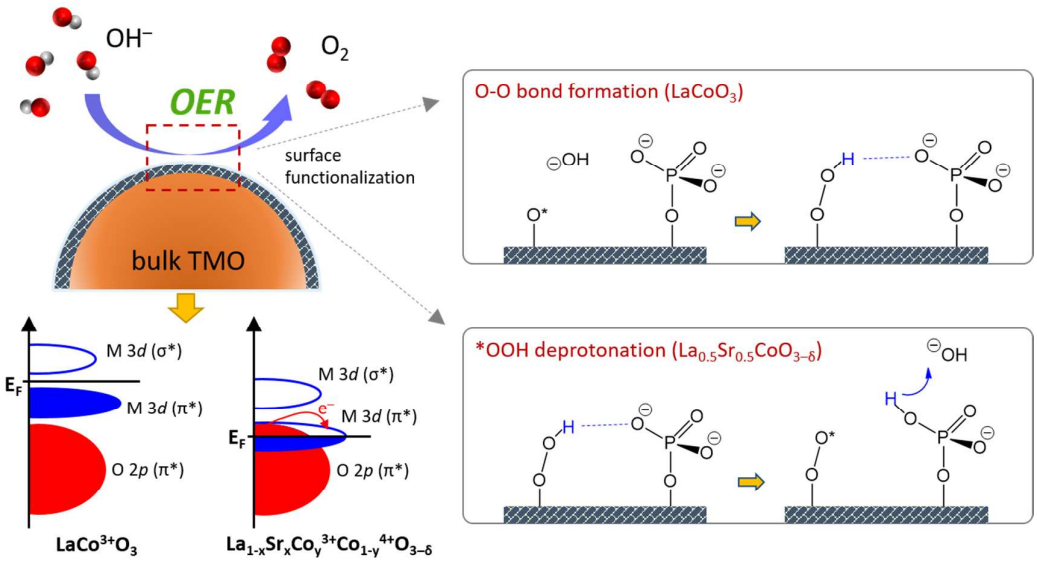

Figure 5. Proposed "dual strategy" and involved mechanisms for improving the OER activity for perovskite catalysts. $LaCoO_3$ is used as a reference example. The bulk electronic structure can be optimized by Sr^{2+} cation substitution to push the O 2*p* band close to the Fermi level. The surface functionalization with Pi groups improves the proton transfer kinetics, assisting the deprotonation step from –OOH to–OO* during the OER.